Flow Characteristics of Double-Cruciform Parachute at Inflating and Inflated Conditions

Fang Ming, *Sun Jianhong* *, *Zhang Tong*, *Hou Bin*, *Zhang Yantai*

Key Laboratory of Aircraft Environment Control and Life Support of MIIT, College of Aerospace Engineering, Nanjing University of Aeronautics and Astronautics, Nanjing 210016, P. R. China.

(Received 29 December 2017; revised 17 November 2018; accepted 5 December 2018)

Abstract: The fluid-structure interaction (FSI) between the canopy and flow field on the inflating and inflated conditions is investigated based on the arbitrary Lagrange-Euler (ALE) method, in both a single- and double-cruciform parachute systems. The projection area of canopy is calculated in the inflation process. The flow field characteristics and the interaction between canopies are analyzed. Results showed that, with free stream velocity of 50 m/s, overinflation phenomenon would not occur during the inflation process of the double-cruciform-parachute system, because the collision and extrusion of the two canopies during inflation obstructed the oscillation of the inner gores. Concurrently, compared with the single-cruciform parachute, the vortex motion in the wake of double-cruciform-parachute is more intense. Thus the double-cruciform parachute system oscillated at a velocity of 50 m/s with an angle of less than 6.8°. By comparison, the oscillation angle of the single-cruciform parachute was within 3.5° at the velocity of 50 m/s. The results are consistent with those of the wind tunnel test.

Key words: process of inflation; arbitrary Lagrange-Euler (ALE); Lamb vector divergence; cruciform parachute

CLC number: V211.3 **Document code**: A **Article ID**: 1005-1120(2018)06-0992-08

0 Introduction

As an aerodynamic decelerator, parachutes, especially cruciform parachutes, are of obvious advantage for their larger resistance coefficient, shorter inflation time, lower opening shock, satisfying stability, and so forth[1]. Excellent deceleration properties enable the cruciform parachutes, both a single parachute and multi-parachute system, to be used as drogue chutes, recovery parachute, and aerial bomb parachute, etc. Compared with the single parachute with a large scale canopy, a multi-parachute system has the advantages of shorter inflation time, easier manufacture, convenient ground recovery, and stable descent performance[2]. However, in a multi-parachute system, there still exist such problems as unsynchronized opening of each canopy, non-uniform distribution of aerodynamic force, etc. To ameliorate these problems, the inflation process and aerodynamic performance of the multi-parachute system have attracted more attention of scholars.

Though wind tunnel test is one of the essential approaches to investigate the inflating process and descent performance of a parachute system, it is difficult to carry out multi-parachute system test in a wind tunnel since the test section of a wind tunnel is relatively small, compared with huge area of canopies. On the other hand, it is also difficult to study fundamental problem theoretically, because the flow field is random, unsteady and nonlinear, and the canopy is made of porous and flexible material. With the advent of computational fluid dynamics (CFD) and upgrading of computer performance, numerical simulation has become an important and widely-used approach to investigating a multi-parachute system. Xu et al.[3] analyzed the canopy contact of a multi-para-

* Corresponding author, E-mail address: jhsun@nuaa.edu.cn.

How to cite this article: Fang Ming, Sun Jianhong, Zhang Tong, et al. Flow characteristics of double-cruciform parachute at inflating and inflated conditions[J]. Trans. Nanjing Univ. Aero. Astro., 2018, 35(6): 992-999.
http://dx.doi.org/10.16356/j.1005-1120.2018.06.992

chute system composed of three C-9 canopies based on the finite element method, and obtained the canopy deformation during the inflation process. Based on the stabilized space-time fluid-structure interaction technique, Takizawa et al.[4-6] numerically simulated two multi-parachute systems containing two and three ringsail canopies, respectively, and attained the geometric shape and flow field of canopy in a stable descent. Besides, Takizawa applied this fluid-solid coupling method further to an annular multi-parachute cluster with a larger structure porosity[7,8]. Guruswamy[9] numerically investigated the unsteady aerodynamic characteristics of a multi-parachute system composed of three circle flat parachutes using an overset grid. Mcquilling et al.[10] reported the influence of suspension lines and payload on overall aerodynamic resistance and flow fields of a double-annulus parachute system. In recent years, more and more attentions have been paid to multi-parachute systems in China. Based on the multi-body system method and the Kane equation, Ke et al.[11,12] analyzed numerically the aerodynamic force, velocity, and displacement of the multi-parachute-payload system. Han et al.[13] used the multi-node statics model to build a geometric model of inflated multi-cruciform-parachute system and studied its aerodynamic features. Based on the ALE method, Lian[14] simulated the stable decent of a multi-ringsail-parachute system and studied the variation of canopy shapes as well as that of the flow field. Fan[15] presented the influence of the contact of canopies on the inflation process of a multi-parachute system by simulating the multi-C-9-parachute system with the membrane-cable-based nonlinear finite element method. It should be noted that the multi-parachute system is mainly composed of circle flat parachute or ring sail parachute, while few results can be found in double-cruciform parachute system as an auxiliary drogue device in airplane landing.

Herein, the fluid-structure interaction of double-cruciform parachute system is simulated by the ALE method. The shape, projected area and the flow field characteristics of the canopies are investigated. Meanwhile, the inflation processes of a single- and double-parachute system are compared. Results can provide a theoretical reference for the design of the double-cruciform parachute system in engineering.

1 Governing Equations

The double-parachute system consists of two same cruciform parachutes, or rather two same cruciform parachute canopies, whose air permeability includes fabric permeability and geometric permeability. The geometric permeability is mainly composed of the permeability caused by apex and the air permeability of slot formed by adjacent gore arms. On the surface of the canopies, reinforcement tapes are sewed, as shown in Fig. 1.

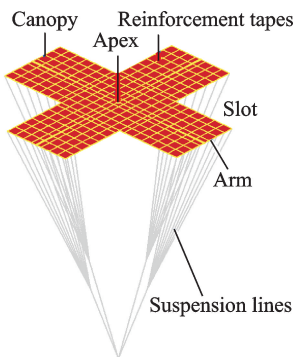

Fig. 1 Configuration of cruciform parachute

The incompressible unsteady flow equations ($Ma<0.3$) based on the ALE method can be rewritten as

$$\frac{\partial \rho}{\partial t}=-\rho\frac{\partial v_i}{\partial x_i}-(v_i-\hat{v}_i)\frac{\partial \rho}{\partial x_i} \tag{1}$$

$$\rho\frac{\partial v_i}{\partial t}=\sigma_{ij,j}+\rho b_i-\rho(v_i-\hat{v}_i)\frac{\partial v_i}{\partial x_j} \tag{2}$$

$$\rho\frac{\partial E}{\partial t}=\sigma_{ij}v_{i,j}+\rho b_i v_i-\rho(v_j-\hat{v}_j)\frac{\partial E}{\partial x_j} \tag{3}$$

where ρ is the air density, v_i the air velocity, $\hat{v}_i$ the grid velocity, b_i the unit volume force, E the total energy of air, and σ_{ij} the stress tensor.

$$\sigma_{ij}=-p\delta_{ij}+\mu(v_{i,j}+v_{j,i}) \tag{4}$$

As a typical nonlinear dynamic model for the canopy with flexible structures and large deformation, the structural governing equation is

$$\rho_s\frac{\mathrm{d}^2x_{si}}{\mathrm{d}t^2}=\sigma_{ij,j}+\rho_s b_i \tag{5}$$

where ρ_s is the fabric density and x_{si} the fabric displacement.

2 Simulation Method and Verification

2.1 FSI method

In the coupling calculation of inflation for cruciform parachutes, how to transfer the calculation results of the last step to the next can be essential in the coupling surface. In each time step, the node forces of the flow field element and the canopy element should be calculated separately, and then the node forces of the fluid-structure interface are coupled by a penalty function. When the penetration happens, it is stipulated that the relative displacement d of the structure and the flow field is the penalty factor. The force on the canopy node is $F_s = k \cdot d$. Here, k is the stiffness coefficient. The node force of the fluid is equal to that of the canopy, though with an opposite direction, i. e., $F_l = -F_s$, as shown in Fig. 2.

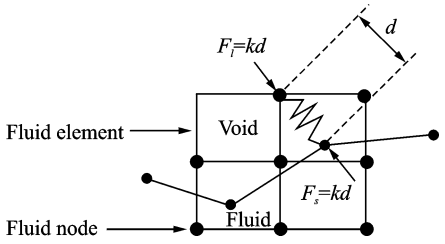

Fig. 2 Penalty method of fluid-structure interaction interface

The FSI numerical solution uses the time-explicit central difference method with the second-order time accuracy by time-marching methodology. Then the velocity and displacement of each fluid and structure node can be calculated by

$$\boldsymbol{u}^{n+1/2} = \boldsymbol{u}^{n-1/2} + \Delta t \boldsymbol{M}^{-1}(\boldsymbol{F}_{\text{ext}} + \boldsymbol{F}_{\text{int}}) \tag{6}$$

$$\boldsymbol{s}^{n+1} = \boldsymbol{s}^{n-1} + \Delta t \boldsymbol{u}^{n+1/2} \tag{7}$$

where $\boldsymbol{u}$, $\boldsymbol{s}$ are the vectors of velocity and displacement, respectively; n is the number of iteration; $\boldsymbol{M}$ is the diagonal matrix of mass; and $\boldsymbol{F}_{\text{int}}$, $\boldsymbol{F}_{\text{ext}}$ are the vectors of internal and external forces, respectively.

2.2 Mesh

The computational domain is $10D_0 \times 7D_0 \times 7D_0$, where D_0 is the nominal canopy diameter of a single parachute. The canopy is located $6D_0$ away from the exit end. For the double-parachute-system, their canopies are divided into 9 216 shell elements. The suspension lines and reinforcement tapes are divided into 9 984 cables. The grid of the flow field near the interface of canopy is locally refined so as to obtain more accurate results. The flow field encompasses 2.44×10^6 hexahedral solids, as shown in Fig. 3. The velocity boundary and the pressure boundary are used at the inlet and outlet, respectively. Besides, the non-reflective boundary is chosen for the surrounding.

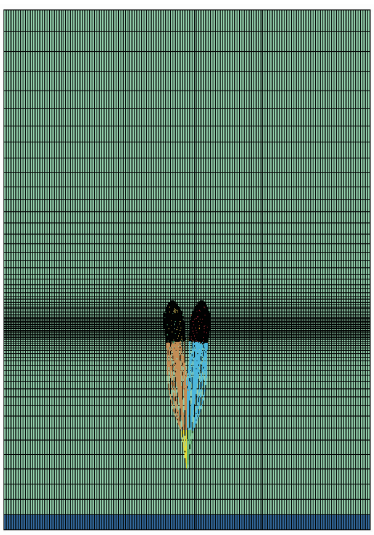

Fig. 3 Fluid domain mesh

The initial shape of the canopy, which is made of the flexible folded fabrics, is extremely complicated in application. It challenges us to precisely build an initial geometric model describing the cruciform parachute under realistic conditions. Inspired by Kim's[16] method, we establish the initial shape of the cruciform parachute. The specific implementation process of the method is that the pull is exerted to the fully extended cruciform parachute, and the shape of parachute in force equilibrium is the initial one of the cruciform parachute. Meanwhile, the pull is the drag force of the retarding parachute at a constant velocity. Based on the method, the initial shape of the single cruciform parachute is rebuilt, as shown in Fig. 4(a). Similarly, the initial shape of the double-cruciform parachute can be provided

by mirroring that of the single parachute, as shown in Fig. 4(b).

(a) Single parachute (b) Double parachutes

Fig. 4 Initial folded states of cruciform parachutes

2.3 Verification

A C-9 parachute[15] is utilized to verify the proposed method. Its diameter of the apex is 0.85 m, and the diameter of the fully extended canopy is 8.50 m. The fabric density of the canopy is 533.77 kg/m^3 with an elastic modulus of 0.43 GPa and Poisson's ratio of 0.14. The canopy is 0.10 mm thick and the suspension lines are 9.00 m long, with a canopy density of 462.00 kg/m^3 and an elastic modulus of 97.00 GPa. The longitudinal reinforcement tapes, with the same material as suspension lines, joint together at the apex of the canopy. The free stream velocity for C-9 is 80 m/s and the atmospheric density is 1.18 kg / m^3. Moreover, the node at the end of the suspension lines is a fixed constraint and the side boundary of flow field is non-reflective.

For a stable fully-extended condition, the ratio of the projected area to the unfolded gore area of the canopy is 0.428, which is close to the numerical result of 0.4036 in Ref. [15]. The canopy shape of the inflated C-9 is similar with that of the test results[17], as shown in Fig. 5.

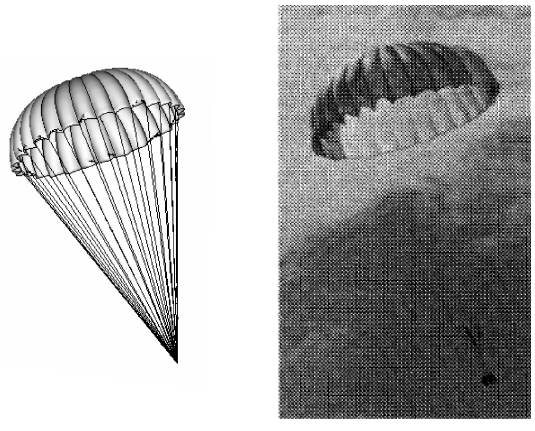

(a) Simulation result (b) Test result[17]

Fig. 5 Comparison of numerical and experimental results of inflated C-9 parachute[17]

3 Results and Discussion

3.1 Change of canopy shape

For the double-cruciform parachutes, there exist the canopies collision and extrusion in the inflation process. In the extreme case, it will lead to a disable inflation. Thus, it necessitates the detailed analysis of the canopy shape change during the inflation process for the double-cruciform parachute. To understand the characteristics of inflation process, we simulated the inflation processes of single- and double-cruciform parachutes under the same working conditions. The free stream velocity during the cruciform parachute inflation process is 50 m/s, which is in the range of the landing velocity of the aircraft.

The canopy shapes during the inflation processes for the single- and double-cruciform parachutes are shown in Figs. 6 and 7, respectively. The single parachute inflation processing was presented, from the unfolding (Fig. 6 (a)), expanding in the crown expeditiously (Fig. 6 (b)), overinflation phenomenon (Fig. 6 (c)), and to stable inflated shape with flapping in a small angle (Fig. 6 (d)). Furthermore, the evolution of the double-cruciform parachute shape is similar to that of the single cruciform. However, for the double-cruciform parachute, the obvious overinflation phenomenon was not been observed. Since the collision and extrusion of the two canopies during the inflation obstruct the oscillation of the inner gores, the overinflation of the canopies is suppressed during the adjustment of the contact-separation-recontact process of the double parachutes, as shown in Figs. 7 (b-d). In addition, the rolling angle of each parachute around its axis varies during the inflation process. Here, we define the oscillation angle of the single-parachute system as the angle between the central axis of

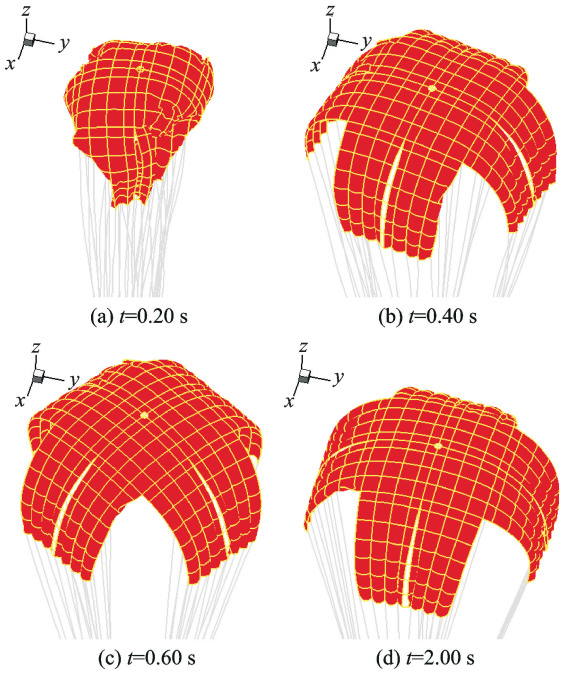

Fig. 6 Canopy shapes of single-cruciform parachute in the inflation process at 50 m/s

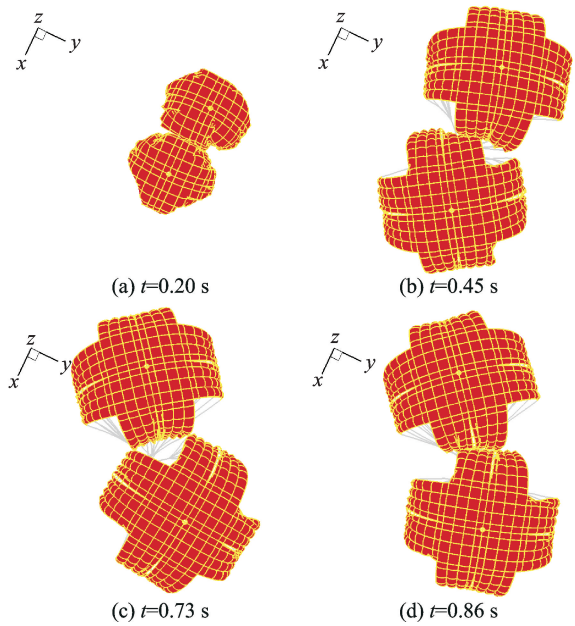

Fig. 7 Canopy shapes of double-cruciform parachute in the inflation process at 50 m/s

the single-parachute and the Z axis, and also define the oscillation angle of the double-parachute system as the angle between the line segment OO' and the Z axis, as shown in Fig. 8, where P_1 and P_2 are the center of the apexes for the double parachutes, and O' is the midpoint of the line segment P_1P_2. When the canopy is inflated, the oscillation angle of the single-fparachute system is within 3.5°, whilst that of the double-parachute system is within 6.8°. In wind tunnel test, the oscillation angle of the single-parachute system is within 3.8°, whilst that of the double-parachute system is within 9.4°. Thus it can be seen that the single-parachute system is more stable than the double-parachute system, and the numerical simulation results agree with those of the wind tunnel test.

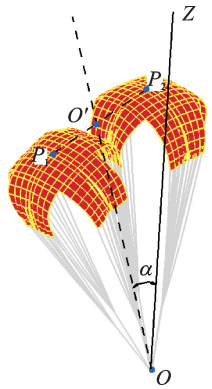

Fig. 8 Schematic for the swing angle of double-parachute system

Fig. 9 shows the variation of projected area of canopy, where a dimensionless projected area A/A_0 represents the ratio of the instantaneous drag area to the fully extended projected area. Besides, the projected area curves show that overinflation phenomenon happens in the inflation process of single parachute, but not obvious in that of double-parachute. When the parachutes are inflated and stable, the projected area ratio of the single parachute is larger than that of the double-parachute, which is mainly due to the collision and extrusion of the two canopies.

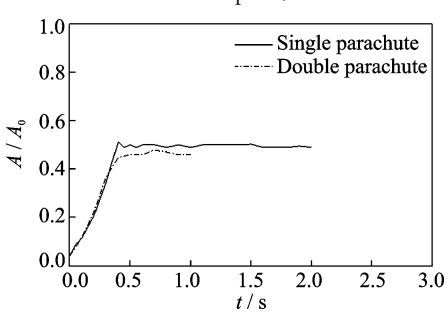

Fig. 9 Projection area of canopy

3.2 Change of flow field

The Lamb vector $\boldsymbol{L}$ is introduced to analyze the shape and attitude ($\boldsymbol{L}=\boldsymbol{\omega}\times\boldsymbol{u}$, where $\boldsymbol{\omega}$ is the vortex vector and $\boldsymbol{u}$ is the velocity vector). The

Lamb vector is a vortex force, which is conducive to understand the flow characteristics of the flow field around the canopy. The divergence of Lamb vector can be used to study the dynamic process in the flow field. Lamb vector divergence $\nabla \cdot \boldsymbol{L}$ can be written as

$$\nabla \cdot \boldsymbol{L} = \boldsymbol{u} \cdot \nabla \times \boldsymbol{\omega} - \boldsymbol{\omega} \cdot \boldsymbol{\omega} \tag{8}$$

where $\nabla \cdot \boldsymbol{L} > 0$ and $\nabla \cdot \boldsymbol{L} < 0$ mean that the momentum transport is dominated by the deformation and the vorticity pushing, respectively, whilst $\nabla \cdot \boldsymbol{L} \approx 0$ means that the deformation and vorticity pushing are in a state of partial equilibrium. Therefore, the momentum transport format in the flow field is qualitatively judged by the sign of $\nabla \cdot \boldsymbol{L}$.

Figs. 10 and 11 show the Lamb vector divergence distribution of the flow field around the single and double parachutes, respectively, where the solid line represents the positive value and the dotted line the negative one. For the single parachute, there is an obvious shear layer in the outer flow field around the canopy (Figs. 10 (a), (b)), and the shear layer has not fully developed, which causes easy momentum exchange between the high-velocity airflow outside the canopy and the airflow near the wake region. Meanwhile, there is also a momentum exchange between the canopy and the airflow, which leads to the formation of a low-pressure region in the wake. Finally, the overinflation is caused in the single parachute inflation process. In the double-parachute inflation process (Figs. 11 (a), (b)), the shear layer of the flow field around the inner gores and the contact of the inner gores hinder the momentum exchange between the inner airflow and the airflow in the wake, as well as the momentum exchange between the canopies and the airflow in the wake. Therefore, the pressure in the wake is larger than that of the single-parachute inflation process,

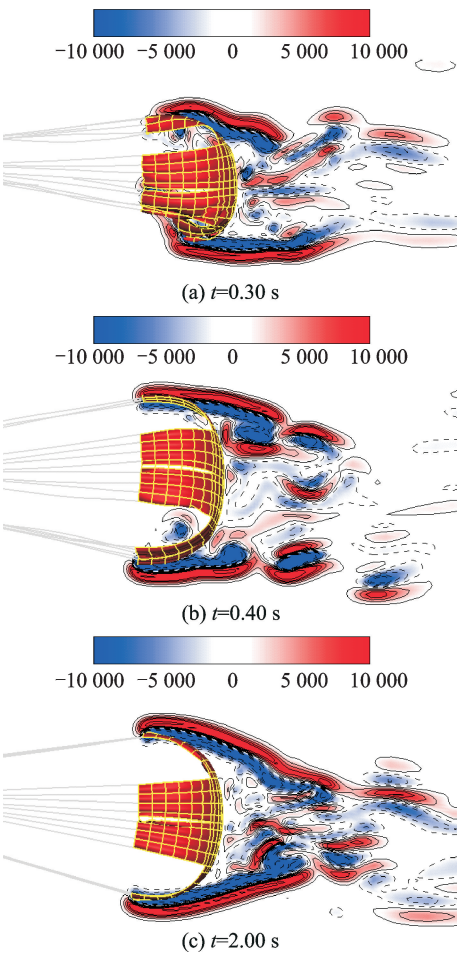

Fig. 10 Lamb vector divergence distribution in flow field of single parachute

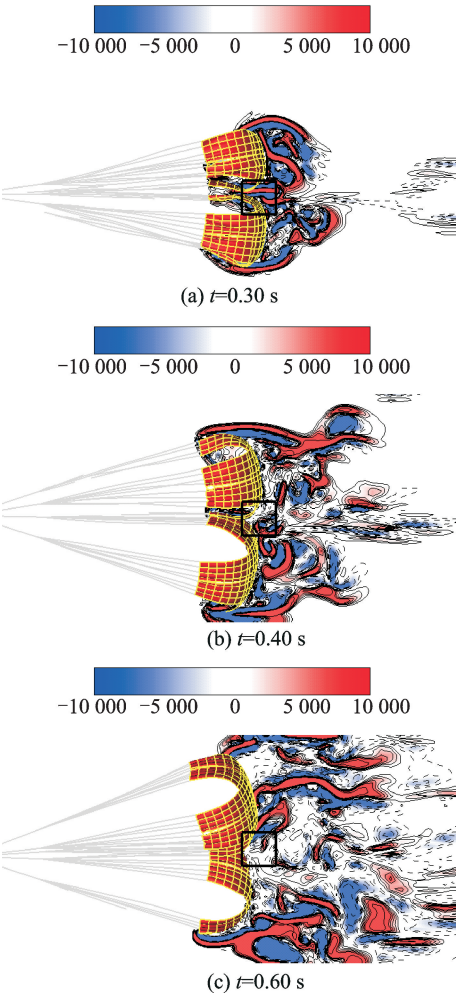

Fig. 11 Lamb vector divergence distribution in flow field of double parachutes

leading to the phenomenon that overinflation was not been observed in the double-parachute. When the canopy is inflated, for the single parachute, the shear layer of the flow field around the canopy is fully developed, which makes the momentum exchange in the wake stable. But for the double-parachute, the momentum transport format of the flow field around the inner gores is changing, and the shear layer is failure, which strengthens the momentum exchange between the inner airflow and the wake flow. Meanwhile, the vortex motion in the wake is intense. When the flow field reacts on the double-parachute, the attitude of the parachutes is changed, which causes a larger oscillation angle of the double-parachute system, compared with that of the single-parachute system.

4 Conclusions

The fluid-structure interaction in both the single- and double-cruciform parachute systems is simulated based on the ALE method. The canopy shape and flow field are analyzed and the following conclusions can be drawn as follows:

(1) With the given parameters, the collision and extrusion of the two canopies obstructed the oscillation of the inner gores, and the momentum exchange in the wake of the single cruciform parachute is more intense. It explains why overinflation is not observed in the inflation process of double-cruciform parachute system, but in that of single-cruciform parachute.

(2) When the canopies are inflated, the vortex motion in the wake of double-cruciform parachute is more intense, compared with that of single-cruciform parachute. The flow field affects the canopies, making the attitude of double-cruciform parachute adjusted continuously. The oscillation angles of single- and double-cruciform parachute systems are within 3.5° and 6.8°, respectively, which agree with the results of the wind tunnel test.

Acknowledgements

This work was supported in part by the Aeronautical Science Foundation of China (No. 20172952031), the Aeronautical Science Foundation of China (No. 20142952026) and the Priority Academic Program Development of Jiangsu Higher Education Institutions (PAPD).

References:

[1] HAN Y H, YANG C X, XIAO H J, et al. Development history and expectation of cross parachute[J]. Ordnance Industry Automation, 2013, 32(3):3-8.

[2] LEE C K, SADECK J E. Controlled opening method for clustered parachute [J]. Journal of Aircraft, 1992, 29(2):264-272.

[3] XU Z L, ACCORSI M, LEONARD J. Simulation of dynamic contact problems in parachute systems[J]. Journal of Aerospace Computing Information and Communication, 2004, 1(7):288-307.

[4] TAKIZAWA K,WRIGHT S, MOORMAN C, et al. Fluid-structure interaction modelling of parachute clusters [J]. International Journal for Numerical Methods in Fluids, 2011, 65(1-3):286-307.

[5] TAKIZAWA K, TEZDUYAR T E. Computational methods for parachute fluid-structure interactions [J]. Archives of Computational Methods in Engineering, 2012, 19(1):125-169.

[6] TAKIZAWA K SPIELMAN T, MOORMAN C, et al. Fluid-structure interaction modelling of spacecraft parachutes for simulation-based design[J]. Journal of Applied Mechanics, 2012, 79(1):010907.

[7] TAKIZAWA K, TEZDUYAR T E, BOBEN J, et al. Fluid-structure interaction modelling of clusters of spacecraft parachutes with modified geometric porosity[J]. Computational Mechanics, 2013, 52(6): 1351-1364.

[8] TAKIZAWA K, TEZDUYAR T E, BOSWELL C, et al. FSI modelling of the reefed stages and disreefing of the Orion spacecraft parachutes[J]. Computational Mechanics, 2014, 54(5):1203-1220.

[9] GURUSWAMY G P. Fast database generation for parachute cluster using Navier-Stokes equations on supercomputers[J]. Journal of Spacecraft and Rockets, 2015, 52(6):1542-1550.

[10] MCQUILLING M W, POTVIN J. CFD simulations of a double-annulus parachute system for cargo airdrops, using inflated shapes informed by photogrammetry [C]//23rd AIAA Aerodynamic Decelerator

Systems Technology Conference. Daytona Beach, FL: AIAA, 2015: 2169.

[11] KE P, YANG C X, SUN X W, et al. Novel algorithm for simulating the general parachute-payload system: Theory and validation[J]. Journal of Aircraft, 2009, 46(1): 189-197.

[12] KE P, YANG C X. A novel algorithm for simulating the general parachute-payload system: Solver and applications[C]//21st AIAA Aerodynamic Decelerator Systems Technology Conference and Seminar. Dublin, Ireland: AIAA, 2011: 2582.

[13] HAN Y H, YANG C X, XU X D. Multi-node statics model and aerodynamic characteristics of cross parachute clusters[J]. Journal of Aerospace Power, 2012, 27(4): 742-748.

[14] LIAN L, WANG Z Y, ZHANG H Y, et al. Numerical simulation of cluster parachute system during steady-state descent phase based on ALE method[J]. Spacecraft Recovery & Remote Sensing, 2014, 35(1): 21-28.

[15] FAN X Y, XIA J. Membrane-cable-based nonlinear finite element method for inflation and contact problem of folded parachute cluster[J]. Acta Aeronautica et Astronautica Sinica, 2016, 37(3): 894-905.

[16] KIM J D, LI Y, LI X L. Simulation of parachute FSI using the front tracking method[J]. Journal of Fluids and Structures, 2013, 37: 100-119.

[17] LEE C K. Experimental investigation of full-scale and model parachute opening[C]//8th Aerodynamic Decelerator and Balloon Technology Conference. Reston: AIAA, 1984: 220.

Mr. **Fang Ming** is currently a Ph. D. candidate of Nanjing University of Aeronautics and Astronautics (NUAA). His research interest focuses on aircraft environment control and life support.

Prof. **Sun Jianhong** received his B. S. and M. S. degrees in Aerodynamics from NUAA in 1989 and 1996, respectively. He received Ph. D. degree in Mechanical Engineering from Hong Kong University of Science & Technology in 2001. His research interests are focused on environmental fluid mechanics and aircraft environment control and life support。

Ms. **Zhang Tong** is currently a Ph. D. candidate of NUAA. Her research interest focuses on computational fluid dynamics.

Mr. **Hou Bin** is currently a Ph. D. candidate of NUAA. His research interest focuses on computational fluid dynamics.

Mr. **Zhang Yantai** is currently a Ph. D. candidate of NUAA. His research interest focuses on computational fluid dynamics, particularly in fluid-structure interaction areas.

(Production Editor: Wang Jing)